Spectroscopic Investigations of Mining Residues Drying Kinetics to Predict and Prevent Fugitive Dust Emission

Gilles-Alex Dessap Pefete[1], Josée Maurais[2] and Patrick Ayotte[3]
1. PhD Candidate
2. Postdoctoral Fellow
3. Professor
Sherbrooke University, Sherbrooke, Canada
Corresponding author: gilles-alex.dessap.pefete@usherbrooke.ca
https://doi.org/10.71659/icsoba2024-br003

Abstract

Aluminium oxide extraction from bauxite generates over 3000 tonnes of filtered bauxite residue daily at Rio Tinto's Vaudreuil Plant. Managing these mine tailings includes addressing the risks of fugitive dust scattering from their surface while they are momentarily stored in the open without dust suppressant at the disposal site in Jonquière, Quebec. To mitigate the risks, continuous monitoring of the drying process is imperative. A real-time quantification of their surface moisture content (SMC) is necessary to predict and prevent fugitive dust scattering, thereby reducing managing and mitigating costs. Albedo measurements in the near infrared (λ = 1200–1550 nm) will be shown to be a precise, sensitive and selective optical method for characterizing the mine tailings' SMC and monitoring their drying rate. A portable device has been designed for continuous SMC measurement, with high temporal and spatial resolution allowing their drying rate to be monitored *in situ* and in real time, under adverse environmental and operational conditions. This device also facilitates laboratory investigations into the dependencies of the mine tailings' drying rates on ambient air temperature and relative humidity, revealing how atmospheric boundary conditions influence water transport mechanisms within their interconnected porous network, namely capillary pumping and gaseous diffusion. The drying rates accelerate with increasing temperatures and decreasing relative humidity, while surface drying is more rapid in frozen tailings because capillary pumping is significantly inhibited. A comprehensive and quantitative knowledge of the impact of these key parameters, along with that of meteorological conditions such as wind speed and solar irradiance, and their recent history, should improve our description of water transport mechanisms and kinetics within mine tailing. The quantification of their drying rates should also improve our prediction of the evolution of their SMC and promote the development and implementation of models and tools necessary for the forecasting and prevention of fugitive dust scattering events thereby contributing to the reduction of the environmental impact of the mine tailings disposal site.

Keywords: Fugitive dust, Remote sensing, Surface water content, In situ monitoring, Water transport mechanisms.

1. Introduction

The rapid population growth since the early 20th century has driven a notable increase in global economic activity, with the mining sector experiencing a 58 % rise in demand between 2000 and 2021 [1]. This industrial growth has significantly increased the environmental footprint of the mining sector requiring improved waste and emissions management strategies [2, 3]. For instance, in Canada in 2021, the production of 3.2 million tonnes of aluminium generated approximately 6 million tons of waste [1]. The extraction of aluminium oxide via the Bayer process continues to present a significant challenge for the mining industry, particularly concerning the disposal and storage of bauxite residues, the primary byproduct [4]. Given their large quantities, these residues must often be momentarily stored outside without protection from the elements [4], as they require

to prolong drying times before potential revalorization or revegetation strategies can be implemented [5]. When weather conditions favour the drying of the superficial layers of bauxite residues, these materials become highly susceptible to fugitive dust emissions [6]. This issue is especially critical during winter in boreal regions that harbour seasonal snow covers, as dust deposition on snow can alter its albedo, accelerating melting thus affecting local hydraulic budget management due to snow melt [7, 8]. Fugitive dust emissions from tailings disposal sites could represent environmental and health risks to nearby communities. Exposure to fine particulate matter, such as basic iron oxide particles from bauxite residues, can lead to respiratory complications upon inhalation [6, 9]. This highlights the importance of effective management and mitigation strategies for dust emissions to reduce the environmental footprint and health hazards associated with mining activities.

Several costly and labour-intensive methods are currently employed to control and suppress fugitive dust emissions. These include the use of liquid dust suppressants and the application of sand or wood chip overlayers. However, these methods have significant drawbacks. They not only incur high costs and require substantial labour but also reduce the storage capacity of tailings disposal areas, thereby shortening their lifespan. Additionally, dust suppressants can inhibit bulk evaporation, which is undesirable since slurries need to dry until they reach solid fractions suitable for subsequent on-site geotechnical applications. Excessive use of dust suppressants can hamper evaporation, delaying the revalorization and restoration of disposal sites [5]. In turn, free evaporation from tailings can lead to premature drying of the superficial layers, favouring dust emissions when capillary forces release their grip on dust particles [6, 10]. A delicate balance must thus be struck between the requirements of efficiently attaining sufficiently high drying fractions to allow for proper manipulation and geo-technical compaction on the disposal site, while preventing surface layers from reaching elevated drying states which increases risks of fugitive dust emissions. Predicting the drying state of slurry surfaces is challenging due to the limited understanding of how environmental conditions such as temperature, relative humidity, solar irradiance, and precipitation affect evaporation kinetics. Therefore, there is a need for improved continuous and surface-sensitive monitoring methods to assess tailings moisture content (TMC) for better risk management and dust emission prevention.

To address this challenge, a bauxite residue storage area (BRSA) was selected as a case study for developing remote sensing and on-site monitoring tools. The study involved collecting bauxite residue samples and characterizing their physico-chemical properties, including moisture content [10]. Surface drying states and evaporation kinetics were analysed using surface-specific optical techniques, such as albedo measurements with a field spectroradiometer at short-wave infrared (SWIR) wavelengths, and thermal imaging using an infrared camera. These optical methods need to be validated for their reliability and robustness under the harsh conditions of BRSA operations. They must provide sufficient precision, accuracy, surface sensitivity, and selectivity for remote sensing applications. Ideally, these methods should not rely on the highly variable solar irradiance flux as a light source to ensure consistent TMC measurements throughout the complete diurnal cycle and be immune to fluctuations in the nebulosity. In situ methods for estimating soil moisture content, such as gravimetric and dielectric measurements, are limited in several ways. Gravimetric methods, while accurate, are labour-intensive and not feasible for continuous monitoring in the field. Dielectric measurements, which include capacitance and time-domain reflectometry, can be influenced by soil salinity and composition, making them less reliable for heterogeneous materials like bauxite residues [11]. Neutron probes, though effective for volumetric water content measurements, are expensive, require specialized training, and pose safety concerns due to the radioactive source involved [12]. Gamma-ray attenuation methods also provide good volumetric data but suffer from similar drawbacks regarding cost, safety, and complexity [12]. Other remote sensing techniques, such as those using thermal infrared imagery, can provide valuable data but are often limited by atmospheric conditions, which affect the accuracy and reliability of the measurements. These methods are typically not suitable for the

high-resolution, continuous monitoring required for effective dust emission control in bauxite residue storage areas. Therefore, there is a critical need for methods that can provide precise, surface-specific moisture content data in real time, under variable environmental as well as demanding operational conditions.

This study reports recent progress towards the development and validation of portable, sensitive, and non-invasive optical methods for continuous monitoring of moisture content. These methods will provide mining industries with accurate and robust tools for predicting and preventing fugitive dust emissions from tailings storage facilities. By improving risk assessment protocols, these approaches will assist in residue management and environmental mitigation efforts, ultimately enhancing the social acceptability of mining operations. The development of effective monitoring tools for TMC in bauxite residues is crucial for controlling fugitive dust emissions. By addressing the limitations of current methods and leveraging advanced optical techniques, this research aims to provide mining industries with practical solutions for environmental management. The findings from this study will contribute to better predictive models and management strategies for dust emission control, ensuring safer and more sustainable mining practices. The tools developed must eventually be deployable across BRSAs, which usually cover hundreds of hectares. Given the highly heterogeneous, variable, and unpredictable nature of these emissions, robust and adaptable monitoring solutions are essential. By addressing the challenges of monitoring vast and diverse storage areas, this research aims to enhance the effectiveness of dust emission prediction and prevention strategies, thereby reducing the environmental impact and operational costs associated with bauxite residue management.

2. Experimental

2.1 Sample Preparation

Bauxite residues used in this study were sampled at the bauxite residues storage area (BRSA) managed by the Vaudreuil plant of Rio Tinto (Jonquière, Québec). These samples, which underwent filtration at the plant to decrease their water content to approximately 30 %, were neutralized in the laboratory to remove residual caustic, then dried at 137 °C and, finally, finely ground to achieve a homogeneous powder. Two types of samples were prepared: wet residues and frozen residues. The synthetic samples were prepared with an initial volume solid fraction (%VSF) ranging from 60 % to 70 %, calculated using Equation (1). Water and dry bauxite residues were mixed homogeneously to achieve the desired VSF. Frozen samples were covered and thermalized before analysis.

$$\%VSF = m_b/m_t \quad (1)$$

where:

m_b dry bauxite mass, g

m_t wet bauxite total mass, g

2.2 Determination of Surface Solid Fraction (SSF) and Evaporation Rates Using Optical Method

The spectral albedo measurements were conducted using an ASD FieldSpec 4 spectroradiometer from Malvern Panalytical. This instrument has a spectral range from 350 nm to 2500 nm, with a resolution varying from 6 nm to 10 nm between 1400 nm and 2100 nm. The analyses were carried out in reflectance mode after calibration with a 100 % reflectance spectralon (which defines an albedo of 1 across the whole spectral range). Albedo, defined as the ratio of reflected radiation from the sample surface to that of the spectralon, was measured in the laboratory using a 10 W Quartz Tungsten-Halogen Bulb (QTHB10) as the light source, positioned 20 cm above the sample surface, covering an emission range of 400 nm to 2200 nm ($T_{source} \approx 2800$ K). The spectral

irradiance reflected from the spectralon and the sample were collected using an optical fibre located 25 cm from the samples surface, providing measurements with a 60° field of view, and the spectrum was acquired using an InGaAs TE-Cooled photodiode. The device operated at a scanning speed of 100 milliseconds per scan, averaging 20 scans to obtain one spectrum per minute. The spectral albedo of the bauxite residue samples having a specific initial VSF, along with the time-evolution of their VSF, established simultaneously through gravimetric measurements, were analysed in the laboratory using the field spectroradiometer. A differential, or relative, albedo (ΔA, or A_{rel}) was calculated using the samples and spectral albedo at 1200 nm and 1450 nm as shown in Equations (2) and (3), allowing the instantaneous SSF to be determined, and the samples surface drying kinetics to be tracked.

$$\Delta A = A_{1200} - A_{1450} \quad (2)$$

$$A_{rel} = A_{1450}/A_{1200} \quad (3)$$

where:

ΔA differential albedo
A_{rel} relative albedo
A_{1200} albedo intensity at 1200 nm
A_{1450} albedo intensity at 1450 nm

In order to overcome the limitations of the field spectroradiometer for continuous in-situ measurements at the BRSA, a portable near-infrared (NIR) sensor named IRDI (InfraRed Double Irradiance) was developed. This device utilizes dedicated internal light sources, a collimating tube and detectors to capture the reflected signal. The device allows for accurate measurements under challenging environmental and operational conditions and was calibrated for a range of SMC.

The drying kinetics of the wet bauxite residue samples were monitored simultaneously using the thermal imaging methodology described previously [13]. Measurements were carried out using a FLIR® Model A320 thermal camera. This optical technique displays good sensitivity and selectivity [10] and provides accurate real-time monitoring of the evaporation process from the surface of mine tailings by monitoring evaporative cooling at the samples surface which was shown to be a valuable proxy for the evaporation rates [13]. The camera captured temperature variations on the samples surfaces at regular intervals, providing detailed insights into the drying process. All measurements were carried out at controlled temperatures in an environmental chamber (TestEquity Chambers TE-1007C) and at controlled relative humidity using saturated salt solutions. The experiments were chosen to provide a good representation of the environmental conditions, namely air temperatures and relative humidity levels encountered year-round at the BRSA. During all experiments, the weight change of the samples was continuously monitored allowing to capture the drying kinetics of the whole sample, while its SSF was simultaneously monitored with the spectroradiometer and the IRDI, and while the evaporation flux from its surface was concomitantly monitored using thermal imaging [13].

3. Results

3.1 Spectroscopic Analysis of Bauxite Residues

Analysis of the spectral albedo from bauxite residue samples reveals distinct features attributable to water absorption bands. A representative spectrum from a sample with 65 % initial VSF is shown in Figure 1a in red, highlighting characteristic water absorption bands at 1450 nm and 1900 nm. The former is associated with overtones of the symmetric and asymmetric stretching vibrations, while the latter is assigned to combinations of bending and stretching vibrations of water, respectively [14, 15]. Additionally, a less pronounced absorption band centered at around 900 nm was observed, which is attributed to iron oxides such as hematite (Fe_2O_3) and goethite (α-FeOOH), compounds that remain insoluble through the Bayer process. Frozen samples exhibit

similar absorption bands, with systematic but subtle variations in position and intensity due to the phase change between liquid and solid states of water. Albedo measurements of samples prepared with various initial VSF enable changes in spectral intensity of these features to be correlated with the samples VSF, if water is distributed homogeneously within the sample volume. The raw albedo spectra in Figure 1a demonstrate how spectral albedo changes with VSF. While spectral albedo varies monotonously with VSF, the albedo of samples at 75 % SF is inferior to that of samples at 65 % SF in certain regions. This was attributed to the presence of surface water layers resulting from sedimentation and non-uniform reflection due to the heterogeneous surface of the samples [15]. However, the intensity of the characteristic spectral bands of water, such as the one at 1450 nm, showed a continuous monotonous decrease in intensity with increasing SF. This trend indicates specific changes in light diffusion and absorption by interstitial water that varies systematically with VSF. The normalized spectral data in Figure 1b highlights the changes in intensity of the absorption bands of interest around 1450 nm and its dependence with VSF. Considering the general albedo fluctuations caused by sedimentation and sample heterogeneity, a continuous monitoring of either the differential albedo (ΔA), or the relative albedo (A_{rel}), calculated from spectral albedos at 1200 nm and 1450 nm, was chosen to track the drying kinetics.

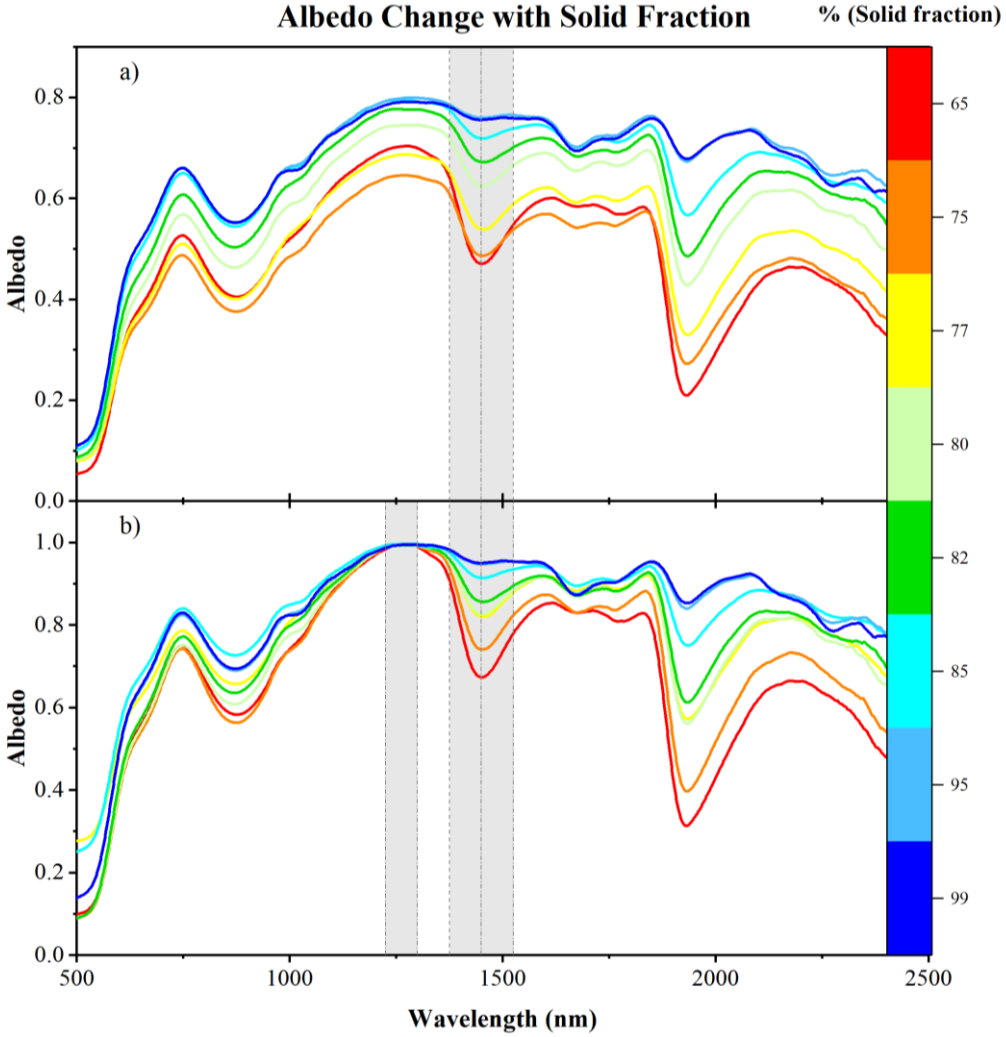

Figure 1. Monitoring of the spectral albedo as a function of the solid fraction. Top (a): Evolution of the spectral albedo on a wet sample at 65 % initial solid fraction, Bottom (b): Normalized spectral albedo data showing absorption bands of interest.

Results from Figure 1 hint at the possibility of using albedo to monitor the evolution of moisture in the residues. This approach offers an alternative method for measuring SSF, overcoming the inherent limitations of other techniques that can only probe the VSF of the samples.

Albedo and gravimetric measurements, taken simultaneously on the same sample were compared to differentiate between surface (SSF) and volumetric (VSF) solid fractions. Albedo measurements were taken from three samples, initially at 65 % VSF but that displayed different thicknesses, in a controlled environment, while gravimetric measurements enabled water mass loss to be tracked. ΔAlbedo values, derived from the sample albedo at 1200 nm and 1450 nm, are shown as a function of VSF in Figure 2. Initially, ΔAlbedo shows a weak dependence on SSF between 65 % and 70 %, a change that is slightly more pronounced in thicker samples due to supernatant layers of water that soon appear at the sample surface due to sedimentation of the solid fraction. This indicates the need to differentiate between surface and volumetric moisture content when using ΔAlbedo measurements. ΔAlbedo decreases non-linearly with increasing VSF, showing a marked decrease between 70 % and 80 %, a less marked decrease between 80 % and 87 %, and stabilization for VSF greater than 90 %. These changes reflect variations in reflection at air/water and water/bauxite interfaces, vibrational absorption, and light diffusion through the porous network as water content decreases. They also confirm the necessity to distinguish between surface and volumetric moisture contents and demonstrate the sensitivity and specificity of spectral albedo measurements to surface dryness. This method shows potential for continuous monitoring of SSF under operational conditions at the BRSA. Indeed, albedo measurements offer high sensitivity and selectivity to the surface, however the field spectroradiometer has important limitations for in situ use due to its high-power consumption and the need for a computer connection for data acquisition and treatment. Furthermore, continuous operation requires frequent recalibration of the field spectroradiometer, resorting to a spectralon that is both fragile and prone to contamination, in addition to requiring an external light source. The device must also withstand harsh conditions at the BRSA and constitute a significant capital investment. All these considerations present impediments for using this methodology for the intended application.

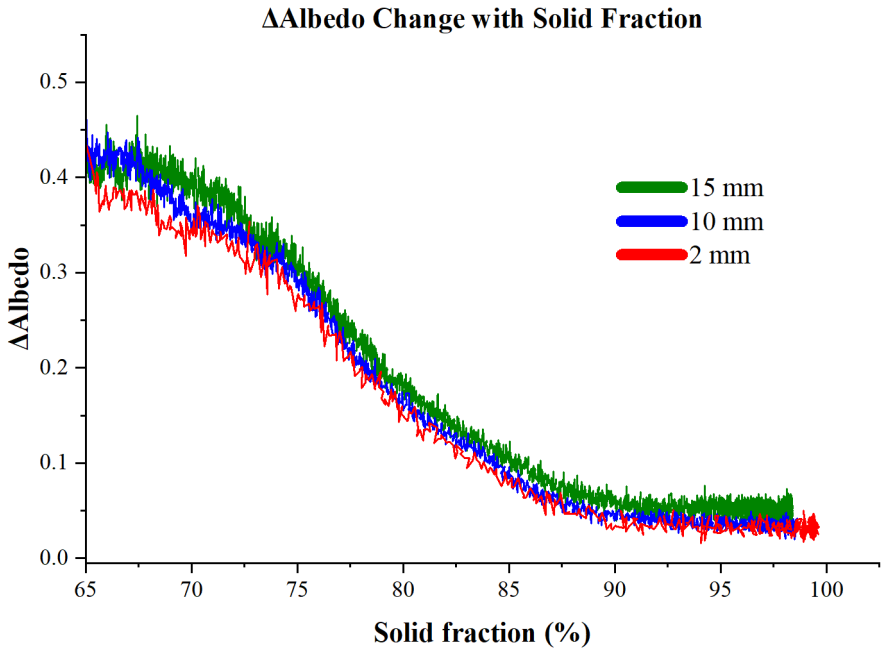

Figure 2. Evolution of the differential albedo (ΔAlbedo) as a function of volumetric solid fraction measured gravimetrically during the evaporation of 3 thicknesses samples at 65 % initial volumetric solid fraction.

These limitations justify the need for developing more economical and robust albedo measurement methods better suited to the adverse operational and environmental conditions at the BRSA. To address these issues, we developed a new optical sensor, the IRDI (InfraRed Dual Irradiance). Similarly to the spectroradiometer, the IRDI allows for reflectance measurements, offering a practical alternative for continuous monitoring of surface moisture content in bauxite residues. The IRDI's functionality relies on the measurement of ΔAlbedo, derived from the total reflected and backscattered intensities from the incident light at 1200 nm and 1450 nm. Although Figure 2 is based on the spectroradiometer measurements, IRDI's ΔAlbedo measurements display the same dependence on VSF but do not require resorting to a spectralon for calibration purposes. This consistency demonstrates that IRDI provides similar surface sensitivity and specificity as those displayed by the spectroradiometer, attributes that become particularly useful, when performed concomitantly with gravimetric measurements, as it enables distinguishing between surface and volumetric moisture contents. This capability suggests that IRDI's ΔAlbedo measurements could potentially provide accurate assessments of surface moisture content in bauxite residue samples. This is demonstrated here by comparing instantaneous SSF analysed using the IRDI with the instantaneous VSF obtained via gravimetric measurements for samples of two different thicknesses, namely 1 mm and 15 mm, subjected to the same evaporation conditions, in Figure 3.

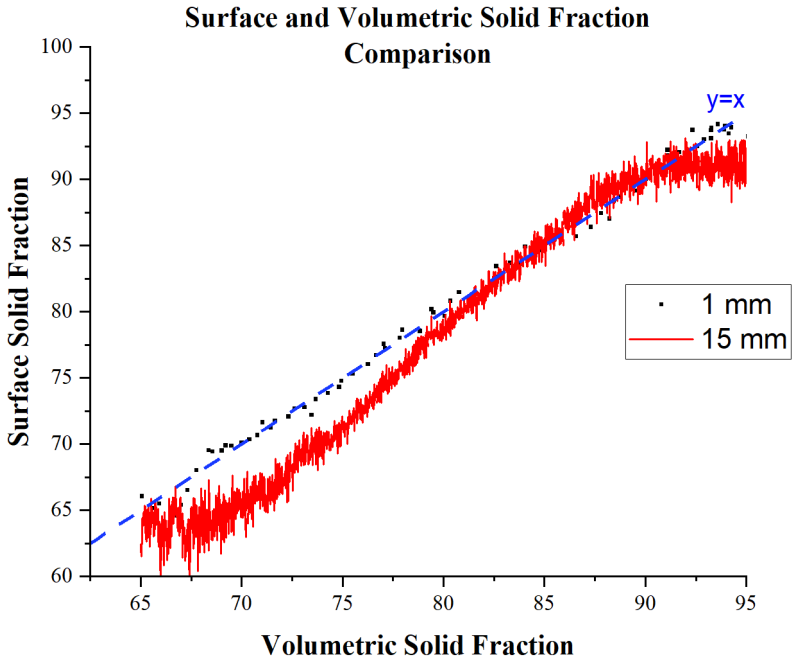

Figure 3. Comparative evolution of the surface solid fraction measured with IRDI, and the volumetric solid fraction measured by gravimetry for 1 mm and 15 mm samples.

For the thinner sample (black dots), SSF is identical to VSF within experimental uncertainty, implying a uniform moisture distribution depth profile. The IRDI's sensitivity enables it to detect ΔAlbedo for thin samples and demonstrates high accuracy in capturing the actual moisture content, as SSF closely matches VSF. In contrast, for the thicker sample (red trace), the surface solid fraction remains independent of the volumetric solid fraction, namely about 64 %, at the beginning of the drying process. This independence is due to sedimentation, which creates a superficial layer of supernatant water. As drying progresses, both SSF and VSF increase until around 90 %, where the SSF remains independent of VSF for the 15 mm thick sample and up to 95 % VSF. This deviation indicates a non-uniform moisture distribution, suggesting that the

surface moisture content does not directly correspond to the volumetric moisture content. The presence of surface water layers resulting from sedimentation affects the IRDI's ability to measure true volumetric moisture content accurately. This highlights the difference in water transport mechanisms between thin and thick samples, showing that moisture content at the surface and the bulk can be different. In thicker samples, the moisture is not evenly distributed throughout the bulk of the sample, and while the IRDI still detects changes in ΔAlbedo as samples dry, the readings primarily reflect surface moisture contents that may differ from the bulk. This non-linearity of the SSF and VSF in thicker samples reported in Figure 3 underscores the IRDI's sensitivity and selectivity to the sample surface. Although the IRDI provides an instantaneous value of SSF, a quantitative assessment of the evaporation kinetics is required to predict the evolution of this parameter as a function of environmental conditions encountered at the BRSA to anticipate fugitive dust emissions. Understanding water transport mechanisms under diverse environmental conditions, ranging from the hot and humid summer to the cold and dry winter is crucial for quantitatively assessing the drying kinetics of residues and provide accurate prediction of their impact on SSF and help in risk assessment efforts to prevent fugitive dust emissions.

3.2 Evaporation Kinetics Analysis

Analysing the evaporation kinetics of bauxite residues is crucial for predicting the evolution of SSF. Figure 4 lists the various parameters measured in the air, at the surface, and within the bulk/subsurface of bauxite residues at the BRSA and that may influence this process. Air temperature and relative humidity are very strongly coupled to the surface of mine tailings and thus, have a very strong and rapid impact on SSF. In turn, soil temperature, volumetric water content, and conductivity reveal internal humidity conditions that are comparatively more weakly coupled to the sample surface and therefore, induce a slower response in SSF. The right-hand side of the graph illustrates how different kinetics, influenced by environmental parameters, affect SSF variations relative to a critical SSF, the threshold where fugitive dust emission risks to reach a critical value. Understanding these kinetics is thus essential for predicting the time scale under which residues should be expected to reach this critical level.

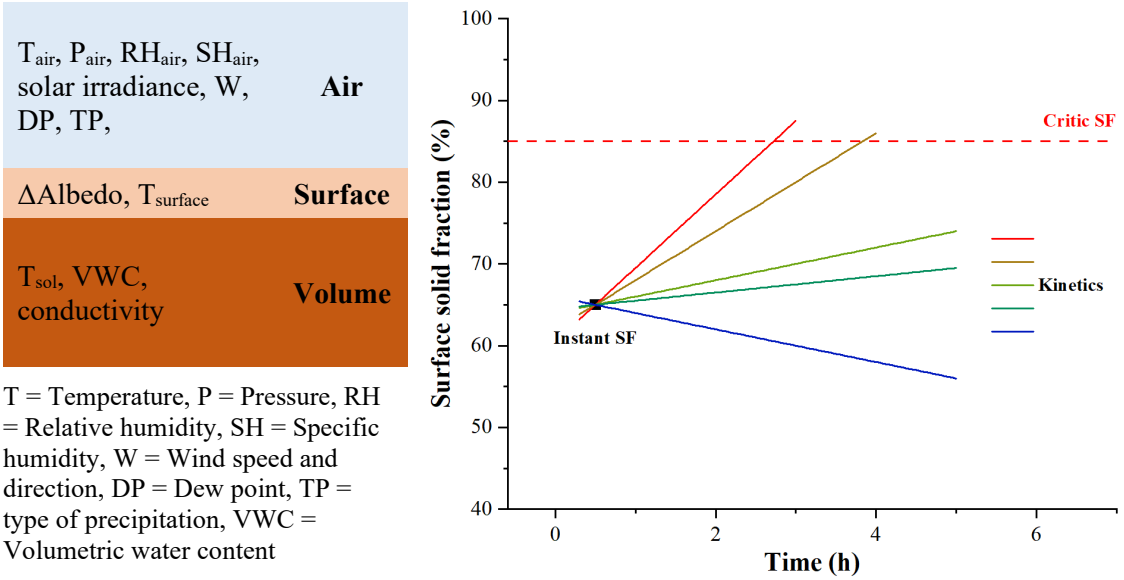

Figure 4. Evaporation kinetics and surface solid fraction prediction of bauxite residues. Left: environmental factors influencing drying kinetics, Right: drying kinetics and critical thresholds for surface solid fraction.

Previous studies on bauxite residues evaporation kinetics have identified two main water transport mechanisms. Initially, after the sedimentation-induced supernatant water layer dries, capillary pumping enables an elevated evaporative flux from the surface to be sustained. Capillary pumping through the residues porous network morphology and interconnectivity is highly efficient, enabling rapid drying as long as hydraulic continuity, which depends on volumetric water content, is maintained [10]. As shown in Figure 5, during this rapid drying phase, the VSF increases quickly and linearly, indicating zero-order kinetics where the drying rate is independent of the sample's VSF. While water is continuously supplied to the surface by capillary pumping allowing rapid evaporation kinetics to be sustained, the rate limiting factor being heat supply through thermal conductivity which occurs thanks to evaporative cooling which reduced sample surface temperatures. However, when the water content drops below the level needed to maintain hydraulic continuity, the residue transitions to a slower, diffusive transport mode, where drying proceeds by gas diffusion through the interconnected porous network of the dry interfacial layer. This transition significantly decreases the slope of the drying curves, inhibiting the evaporation kinetics in the final stages of the drying process. Figure 5 highlights the solid fraction as a function of time for samples of different thicknesses. Thicker samples retain water longer, delaying the transition to the slower diffusive transport mode, while thinner samples transition earlier into the slow diffusive regime. Regardless of the regime, the evolution of the water concentration gradient is crucial for predicting SSF. These observations clearly indicate that capillary pumping initially predominates, drawing water to the surface until hydraulic continuity to the sample surface is compromised. Then, diffusive transport takes over, characterized by slower evaporation rates and a more moderate solid fraction increase, as it must proceed through much slower gas diffusion within the matrix interconnected pore structure.

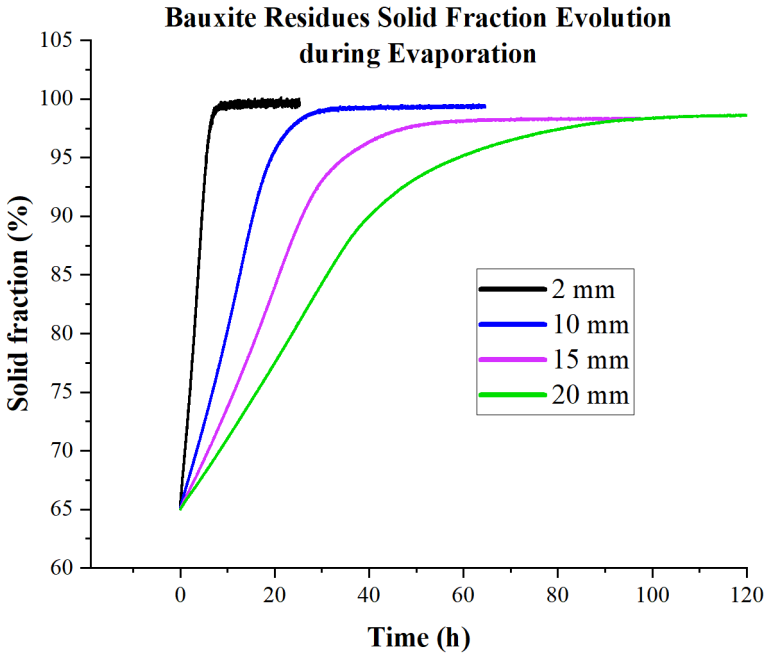

Figure 5. Evolution of solid fraction measured gravimetrically during the evaporation of bauxite at 65 % initial solid fraction with 1, 10, 15 and 20 mm thickness.

Thermal imaging of the samples surfaces presents signatures of these two distinct water transport mechanisms as they present distinctive features that result from evaporative cooling. By analysing the temperature difference between the surface and a reference point, we can observe distinct phases of water transport, as shown in Figure 6. Initially, the temperature difference (ΔT) remains stable, indicating constant evaporation rate and sustained water flux to the surface via capillary action, resulting in a rapid, linear increase in the sample SF. As drying progresses into the

diffusive regime, ΔT increases, signalling the loss of hydraulic continuity and the transition to diffusive transport. Water movement during this slower phase is driven by vapor diffusion within the sample matrix, causing a slower drying rate and thus, an ever-decreasing ΔT. In the subsequent phase, the drying rate decreases significantly. The solid fra0ction continues to increase, but at a slower pace, indicating that drying rates are strongly suppressed by slow diffusive transport. Figure 6 clearly delineates the capillary pumping and diffusive transport stages. The red region represents the capillary pumping phase, where water is actively transported to the surface, and the green region represents the diffusive transport phase. The thermal imaging results corroborate the findings from gravimetric measurements, illustrating the distinct phases of water transport in bauxite residues. Understanding these mechanisms is crucial for predicting drying behaviour and managing fugitive dust emissions in bauxite residue storage areas.

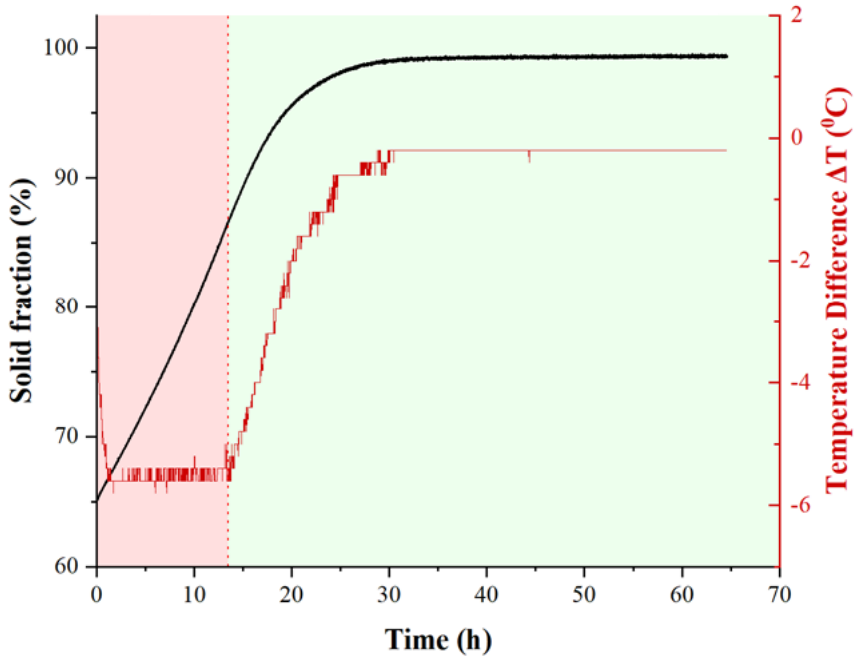

Figure 6. Solid Fraction and Surface Temperature Evolution during evaporation of bauxite at 65 % initial solid fraction with 10 mm thickness.

3.3 Phenomenology of Capillary Transport in Porous Media

Water transport mechanisms in bauxite residues are influenced by several distinct forces. Initially, capillary pumping is governed by Jurin's law, as shown in Equation (4), which estimates the depth at which capillary forces surpass gravitational forces. This law helps us understand the impact of capillary dimensions, wetting properties, and capillarity on pumping efficiency.

$$L = \frac{2\gamma \cos\theta}{\rho g r} \tag{4}$$

where:

L	Capillary height, m
γ	Surface tension, N/m
θ	Contact angle between the liquid and the residue surface
ρ	Density of water, kg/m^3
r	Capillary radius, m
g	Gravitational acceleration, m/s^2

This relationship is based on the mechanical equilibrium between Laplace's pressure, which creates the pressure difference necessary to raise water inside the capillaries, which opposes, at equilibrium, the hydrostatic pressure from capillary rise. Due to the surface tension gradient and the interconnectivity of the pore network, larger capillaries supply smaller capillaries with fluid during this phase [16]. Next, Hagen-Poiseuille's law describes the volumetric rate (dV/dt) from the laminar flow of an incompressible fluid through a cylindrical conduit. The relation is shown in Equation (5).

$$dV/dt = (\pi r^4/8\eta L)\Delta P \quad (5)$$

where:

ΔP Pressure difference, kg/m.s^2
r Capillary radius, m
η Fluid viscosity, kg/m·s
L Capillary length, m
dV/dt Volumetric flow rate, m^3/s

Viscous dissipation plays a crucial role in opposing resistance to capillary pumping. By combining these forces, a comprehensive evaporation model can be created to describe and predict transport mechanisms in bauxite residues. The Bond number (Bo) is also relevant for understanding bauxite residue evaporation, as it measures the relative importance of gravitational forces compared to surface tension forces: $Bo = \Delta\rho g L^2/\gamma$. A low Bond number indicates dominant surface tension effects, while a high value suggests prevailing gravitational forces.

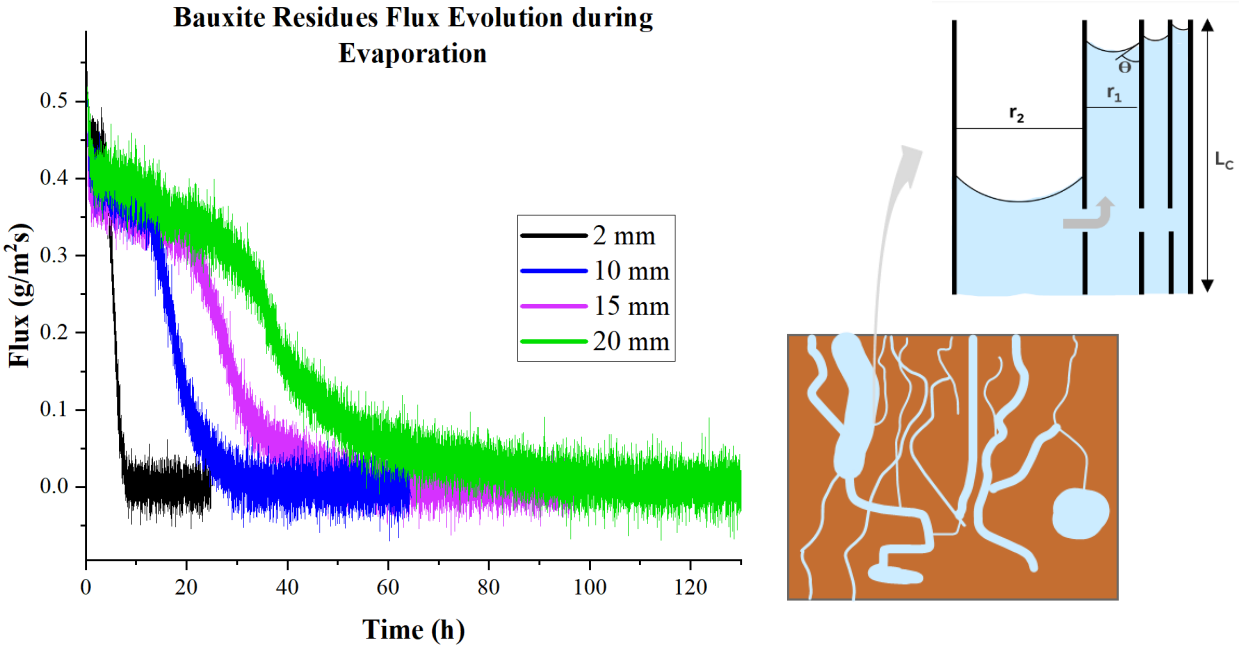

Figure 7. Quantitative and conceptual analysis of bauxite residues drying. Left: evolution of the evaporative flux as a function of time for four sample depths, Right: schematic representation of water transport in capillary networks.

Figure 7 illustrates the evaporative flux calculated from the mass loss of bauxite samples of various thicknesses. During the capillary pumping phase, there is a slight progressive decrease in evaporative flux rather than a constant and sustained flow. This trend is likely related to the distribution of capillary radii, where the finest capillaries, initially responsible for rapid evaporation, see their contribution diminish as surface water evaporates. The figure shows that for thicker samples, the evaporative flux decreases more gradually, indicating that larger

capillaries continue to supply water to the surface even as the finer capillaries dry out. This results in a more extended period of capillary pumping before transitioning to diffusive transport. Thinner samples show a quicker decline in evaporative flux, reflecting an earlier transition to the slower diffusive transport phase. The transition from capillary pumping to diffusive transport is marked by a significant drop in evaporative flux. The figure highlights that the evaporative flux becomes relatively stable during the diffusive transport phase, but at a much lower rate compared to the capillary pumping phase. The critical flux thresholds observed in the figure suggest the effective capillary length beyond which capillary action ceases to dominate. For example, the flux for the 10 mm thick sample drops to about 0.35 g/m²·s, while for the 15 mm and 20 mm thick samples, it drops to around 0.3 g/m²·s. These thresholds correspond to the maximum effective capillary length, indicating a shift from capillary to diffusive transport.

These transport mechanisms are essential for understanding and predicting the evaporation behaviour of bauxite residues based on the structure and morphology of their pore network. It is crucial to determine the maximum capillary length, examine the impact of morphological characteristics on evaporation mechanisms and rates, and develop a model that integrates capillary pumping and viscous dissipation to predict the drying behaviour of bauxite residues. Proper characterization of the sample morphology, such as pore size distribution and interconnectivity, is then essential since these factors significantly impact the water transport phases. Preliminary investigations using the CellStat cold cell [17, 18] and traditional cone beam tomography at 40–150 kV with a focus of 5–40 µm have shown promising results. However, distinguishing lighter phases like water and air remains challenging. Ongoing synchrotron X-ray tomography, which offers enhanced phase contrast capabilities, should help resolve these issues. Ongoing investigations should provide detailed structural and morphological data, including pore size distribution, capillary length, and differentiation between interconnected pore networks and isolated pockets. Understanding these characteristics will enhance the accuracy of predictive models, first on water transport mechanisms in bauxite and second on surface moisture content in relation to environmental parameters influencing bauxite drying kinetics. Ultimately, this will improve predictive models for fugitive dust emissions from the tailings.

4. Conclusion

This study outlines a strategy to acquire a comprehensive understanding of the water transport mechanisms and evaporation kinetics in bauxite residues using spectroscopic techniques and thermal imaging in the laboratory and to develop technologies and methodologies that can be deployed in the field. The findings significantly enhance our understanding of the drying behaviour of bauxite residues, which is crucial for effective dust emission management in bauxite residue storage areas (BRSA).

Using a field spectroradiometer, this study identified distinct water absorption bands at 1450 nm and 1900 nm, corresponding to specific vibrational transitions of water. This spectroscopic analysis enabled the identification of key spectral features related to moisture content in bauxite residues. Albedo measurements provided valuable insights into surface moisture content, showing a strong correlation with gravimetrically measured solid fraction in thinner samples. These investigations demonstrated that albedo can effectively monitor the evolution of moisture content in bauxite residues, offering a reliable method for real-time assessment of surface moisture content which can be different than the bulk in thicker sample. New optical methods like IRDI have shown excellent capabilities for real-time, in-situ measurements of surface moisture content, overcoming the limitations of traditional spectroradiometers. The device's ability to provide instantaneous surface dryness values under challenging environmental and operational conditions is promising for continuous monitoring and management of bauxite residues at BRSAs. The study also underscores the importance of distinguishing between surface and volumetric moisture content in understanding the drying kinetics of bauxite residues. The findings highlight the need

for robust and sensitive measurement techniques to predict drying behaviour accurately and, thus, surface moisture content. Future research will focus on enhancing this predictive aspect of the IRDI device in the field while also exploring water transport mechanisms in greater detail in the laboratory, more specifically in terms of the impact of the structural and morphological characteristics of the tailings interconnected pore network on the drying kinetics.

5. Acknowledgements

We gratefully acknowledge the financial support provided by the Fond de recherche du Québec – Nature et Technologies (FRQNT), Rio Tinto, the Natural Sciences and Engineering Research Council of Canada (NSERC), and the Centre québécois de recherche et de développement de l'aluminium (CQRDA). Additionally, we extend our thanks to Eco Canada for their support. We would like to express our deep appreciation to Jonathan Bernier at CRDA and Stephane Gagnon at the BRSA, as well as CRDA and BRSA staff in Vaudreuil, Canada, for their invaluable contribution in providing bauxite residue samples and for granting access and support to the BRSA. Their assistance was instrumental in the successful completion of this research.

6. References

1. C. Reichl and M. Schatz, Iron and Ferro-Alloy Metals - Non-Ferrous Metals - Precious Metals - Industrial Minerals - Mineral Fuels, *World Mining Data 2023*. https://www.world-mining-data.info/wmd/downloads/PDF/WMD2023.pdf. (Accessed on 29/01/2024)
2. Fridolin Krausmann et al., Growth in Global Materials use, GDP and Population during the 20th Century, *Ecological Economics*, Volume 68 / Issue 10, 2009, 2696-2705, doi.org/10.1016/j.ecolecon.2009.05.007.
3. Robert Ayres and Udo Simonis, *Industrial Metabolism: Restructuring for Sustainable Development*, United Nations University Press, 1994.
4. Adèle Dramou et al., An overview of the mineralogical cCharacterization and treatment strategies of bauxite residues for their sustainable management, *Mineral Processing and Extractive Metallurgy Review*, Volume 44 / Issue 5, 2022, 365–374, doi.org/10.1080/08827508.2022.2064856.
5. B.E.H. Jones, R.J. Haynes, Bauxite processing residue: A critical review of its formation, properties, storage, and revegetation, *Critical Reviews in Environmental Science and Technology*, Volume 41 / Issue 3, 2011, 271–315, doi.org/10.1080/10643380902800000
6. Nkosi Vusumuzi, How mine dumps in South Africa affect the health of communities living nearby, *The Conversation*, Published May 2, 2018. https://theconversation.com/how-mine-dumps-in-south-africa-affect-the-health-of-communities-living-nearby-77113. (Accessed on 30/01/2024).
7. Yulan Zhang et al., Albedo reduction as an important driver for glacier melting in Tibetan Plateau and its surrounding areas, *Earth-Science Reviews*, 2021, 220 :103735, doi.org/10.1016/j.earscirev.2021.103735.
8. Adator Stefanie Worlanyo and Li Jiangfeng, Evaluating the environmental and economic impact of mining for post-mined land restoration and land-use: A review, *Journal of Environmental Management*, Volume 279, 2021, 111623, doi.org/10.1016/j.jenvman.2020.111623.
9. András Gelencsér et al., The red mud accident in Ajka (Hungary): Characterization and potential health effects of fugitive dust, *Environmental Science & Technology*, Volume 45 / Issue 4, 2011, 1608–1615, doi.org/10.1021/es104005r.
10. Josée Maurais, *L'imagerie thermique : Une méthode innovatrice pour mesurer les cinétiques d'assèchement dans les résidus miniers,* 2019. https://savoirs.usherbrooke.ca/bitstream/handle/11143/15796/Maurais_Josee_MSc_2019.pdf?sequence=7&isAllowed=y. (Accessed 02/02/2024)

11. Alessandro Tarantino, Andrew M. Ridley and David G. Toll, Field measurement of suction, water content, and water permeability, *Geotechnical and Geological Engineering*, Volume 26, 2008, 751-782, doi.org/10.1007/s10706-008-9205-4.
12. Pariva Dobriyal et al., A review of the methods available for estimating soil moisture and its implications for water resource management, *Journal of Hydrology*, Volumes 458–459, 2012, 110–117, doi.org/10.1016/j.jhydrol.2012.06.021.
13. Josée Maurais et al., A thermal imaging methodology to study evaporation kinetics in mine tailings, *Environmental Science: Water Research & Technology*, Volume 6 / Issue 5, 2020, 1456–1464, doi.org/10.1039/D0EW00104J.
14. R. J. Gustafsson et al., A comprehensive evaluation of water uptake on atmospherically relevant mineral surfaces: DRIFT spectroscopy, thermogravimetric analysis and aerosol growth measurements, *Atmospheric Chemistry and Physics*, Volume 5 / Issue 12, 2005, 3415–3421, doi.org/10.5194/acp-5-3415-2005.
15. Josée Maurais et al., Monitoring moisture content and evaporation kinetics from mine slurries through albedo measurements to help predict and prevent dust emissions, *Royal Society Open Science*, Volume 8 / Issue 7, 2021, doi.org/10.1098/rsos.210414.
16. Dani Or et al., Advances in soil evaporation physics–A review, *Vadose Zone Journal*, Volume 12 / Issue 4, 2013, 1–16, doi.org/10.2136/vzj2012.0163.
17. Amira Zennoune et al., 3D characterization of sponge cake as affected by freezing conditions using synchrotron X-ray microtomography at negative temperature, *Foods*, Volume 10 / Issue 12, 2021, 2915, doi.org/10.3390/foods10122915.
18. Neige Calonne et al., Study of a temperature gradient metamorphism of snow from 3-D images: time evolution of microstructures, physical properties and their associated anisotropy, *The Cryosphere*, Volume 8 / Issue 6, 2014, 2255-2274, doi.org/10.5194/tc-8-2255-2014.